AEDC-TR-79-87

C-2

A Direct Model Pitch Measurement with a Laser Interferometer Using Retroreflectors

W. H. Goethert
ARO, Inc.

October 1980

Final Report for Period October 1978 – September 5, 1979

Approved for public release; distribution unlimited.

ARNOLD ENGINEERING DEVELOPMENT CENTER
ARNOLD AIR FORCE STATION, TENNESSEE
AIR FORCE SYSTEMS COMMAND
UNITED STATES AIR FORCE

NOTICES

When U. S. Government drawings, specifications, or other data are used for any purpose other than a definitely related Government procurement operation, the Government thereby incurs no responsibility nor any obligation whatsoever, and the fact that the Government may have formulated, furnished, or in any way supplied the said drawings, specifications, or other data, is not to be regarded by implication or otherwise, or in any manner licensing the holder or any other person or corporation, or conveying any rights or permission to manufacture, use, or sell any patented invention that may in any way be related thereto.

Qualified users may obtain copies of this report from the Defense Technical Information Center.

References to named commercial products in this report are not to be considered in any sense as an indorsement of the product by the United States Air Force or the Government.

This report has been reviewed by the Office of Public Affairs (PA) and is releasable to the National Technical Information Service (NTIS). At NTIS, it will be available to the general public, including foreign nations.

APPROVAL STATEMENT

This report has been reviewed and approved.

Marshall K. Kingery

MARSHALL K. KINGERY
Project Manager
Directorate of Technology

Approved for publication:

FOR THE COMMANDER

Marion L. Laster

MARION L. LASTER
Director of Technology
Deputy for Operations

REPORT DOCUMENTATION PAGE	READ INSTRUCTIONS BEFORE COMPLETING FORM
1 REPORT NUMBER: AEDC-TR-79-87	2 GOVT ACCESSION NO
	3 RECIPIENT'S CATALOG NUMBER
4 TITLE (and Subtitle): A DIRECT MODEL PITCH MEASUREMENT WITH A LASER INTERFEROMETER USING RETROREFLECTORS	5 TYPE OF REPORT & PERIOD COVERED: Final Report, October 1978 - September 5, 1979
	6 PERFORMING ORG REPORT NUMBER
7 AUTHOR(s): W. H. Goethert, ARO, Inc., a Sverdrup Corporation Company	8 CONTRACT OR GRANT NUMBER(s)
9 PERFORMING ORGANIZATION NAME AND ADDRESS: Arnold Engineering Development Center/DOT Air Force Systems Command Arnold Air Force Station, Tennessee 37389	10 PROGRAM ELEMENT PROJECT, TASK AREA & WORK UNIT NUMBERS: Program Element 65807F
11 CONTROLLING OFFICE NAME AND ADDRESS: Arnold Engineering Development Center/DOS Air Force Systems Command Arnold Air Force Station, Tennessee 37389	12 REPORT DATE: October 1980
	13 NUMBER OF PAGES: 40
14 MONITORING AGENCY NAME & ADDRESS(if different from Controlling Office)	15 SECURITY CLASS (of this report): UNCLASSIFIED
	15a DECLASSIFICATION DOWNGRADING SCHEDULE: N/A

16 DISTRIBUTION STATEMENT (of this Report)

Approved for public release; distribution unlimited.

17 DISTRIBUTION STATEMENT (of the abstract entered in Block 20, if different from Report)

18 SUPPLEMENTARY NOTES

Available in Defense Technical Information Center (DTIC)

19 KEY WORDS (Continue on reverse side if necessary and identify by block number)

models	retroreflectors
pitch (motion)	optics
measurement	wind tunnels
lasers	environments
interferometers	

20 ABSTRACT (Continue on reverse side if necessary and identify by block number)

A laser interferometer was developed to measure pitch angles of test models in a wind tunnel environment. Small retroreflectors imbedded flush with the surface of the test item provided the necessary reflected light for optical processing of pitch information. The first tunnel measurements indicated pitch measurements could be made providing the retroreflectors remained illuminated with the expanded laser beams. Because of the axial motion of the

DD FORM 1 JAN 73 1473 EDITION OF 1 NOV 65 IS OBSOLETE

20. ABSTRACT (Continued)

model relative to the optics systems, provisions for scanning the laser beams to follow retroreflector motion was incorporated. Using an actual test model, data were taken demonstrating this tracking capability. Calibration data were also taken comparing the interferometer data with the tunnel standard inclinometer.

AFSC
Arnold AFS Tenn

PREFACE

The work reported herein was conducted by the Arnold Engineering Development Center (AEDC), Air Force Systems Command (AFSC), and M. K. Kingery was the Air Force project manager. The results of the research were obtained by ARO, Inc., AEDC Division (a Sverdrup Corporation Company), operating contractor for the AEDC, AFSC, Arnold Air Force Station, Tennessee, under ARO Project No. P32L-02A. The manuscript was submitted for publication on October 5, 1979.

The author wishes to acknowledge the efforts of Gary Johnson in greatly assisting with the tunnel installation and the operation of the optical system before and during the test problem. Special thanks go to Bruce Bomar who was responsible for electronic acquisition and processing of the data.

CONTENTS

ILLUSTRATIONS

TABLE

APPENDIXES

1.0 INTRODUCTION

Wind tunnel model position is commonly determined from a direct reading of the model sting positioning mechanism. Because of aerodynamic loading of the model, significant errors may be encountered because of the deflection of the model force balance and the sometimes lengthy model sting support mechanism. Static loading of the sting and the model balance before a tunnel test produces deflection coefficients to be used when the model is subjected to the aerodynamic loading of the airstream. This technique is a time-consuming procedure both in establishing these deflection coefficients and in the calculation of the model position when large model oscillations prevail.

Ideally, it would be desirable to measure the model angle directly, independent of sting and balance deflections, and by means of an appropriate readout, instantly displaying or recording model position. The objective of this program has been to develop an optical interferometric technique to perform such a measurement.

This development program is based on a laser interferometric technique set forth under a previous project which established an optical system and explored data processing techniques for high resolution distance measurements. Results of that effort are summarized in Ref. 1. The effort here was to establish the pitch measurement technique under actual tunnel conditions for a pitch range of -5 to +40 deg with a resolution of 0.001 deg. The development effort was subdivided into two major tasks in order of priority. Task 1 dealt with measurements concerning model pitch under a relatively idealistic condition. This task deals specifically with making pitch measurements in a wind tunnel environment using small retroreflectors to reflect the light to a detector to sense the model motion. When light is not reflected from a mirrored surface like the retroreflector (a combination of mirrors), the reflection is said to be diffuse in that the reflected light becomes random and possesses a spatial distribution dependent on the nature of the light reflecting surface. Task 2 deals with this more difficult problem of reflecting the light from the model surface directly, thereby requiring added sophistication in the measurement technique because of the substantial loss of laser coherence and received light intensity.

Since what is learned in Task 1 is directly applicable to Task 2, many problem areas could be dealt with independent of the added disturbances associated with the diffused light scattering process. Specifically, vibration and accoustic levels could be assessed and density fluctuations in the airstream caused by shock waves, boundary layers, and so forth could be monitored as to their effects on the interferometric measurement. This report deals primarily with those problems associated with Task 1.

2.0 PITCH MEASUREMENT WITH FIXED OPTICS SYSTEM

To establish the operating capabilities of a laser interferometer for pitch measurements in a wind tunnel environment, a series of proof-of-prinicple test runs was conducted in the Arnold Engineering Development Center (AEDC) Propulsion Wind Tunnel (16T). Pitch measurements for both air-on and air-off were undertaken by attaching the retroreflectors on a contoured plate just behind the model. The attachment point of the retroreflectors was chosen (1) to establish measurement capabilities in a high-turbulence area, (2) to ensure free access to the test section independent of the user model, and (3) to avoid drilling holes in the model for in-house experimental efforts.

2.1 MEASUREMENT TECHNIQUE

The model pitch determination is based on measuring the relative distance between the two optical arms of an interferometer. If the hypotenuse of a right triangle is known, a determination of one of the sides of the triangle will allow calculation of an angle. Reference 1 describes the details of the interferometer system that measures the path length change between the two optical arms of the interferometer. Figure 1 is a schematic illustrating the technique used for the model pitch measurement. The pitch angle is determined by knowing R, the radial distance from the model rotation point to the outermost retroreflector. A data processor directly provides the measurement of the opposite side of the right triangle by fixing one optical arm of the interferometer on a fixed structure of the tunnel wall or some part of the optics package as shown by the alternate measurement shown in the insert of Fig. 1. The model angle is calculated by

$$\alpha = \sin^{-1} \frac{\Delta x}{R} \tag{1}$$

where Δx is the measured change in optical distance. This path length change, Δx, is provided by a digital data processor described in Ref. 1, which counts digital pulses derived from surface motion in discrete steps of $\lambda/4$ where λ is the laser wavelength. Reference 1 also discusses the measurement over a large angular range by using expanded laser beam diameters (the optical arms of the interferometer) to ensure that the retroreflectors remain illuminated through the angular measurement.

For wind tunnel application, passing one laser beam onto the model and leaving the other beam (sometimes termed reference beam) outside the airstream makes the measurement sensitive to density fluctuations which cause index of refraction changes as discussed in Ref. 1. This problem is easily avoided by passing both the sensing beam and the reference beam onto the model. If the beams are near each other and in the plane of the airflow, the same density fluctuations are seen by both beams. The pitch angle is now

calculated by replacing R with S, shown in Fig. 1, where S is the spacing between the two beams. The change in path length will now be $\Delta x'$ with S the new hypotenuse. Passing both beams onto the model provided an added advantage in that the point of model rotation need not be fixed relative to the optics package.

Since the interferometer measures the relative change in optical path length between the two light beams, a known reference angle is required. The zero angle-of-attack position, set with a standard inclinometer, is used for this purpose. In Tunnel 16T, fogging conditions at the beginning of the test are usually severe enough to extinguish the laser beams causing loss of the reference angle set with the standard inclinometer. However, with the aid of the model force balance the accuracy of the zero angle of attack is still maintained. An alternate optical measurement technique establishing an absolute angle reference is presently under evaluation. This technique utilizes a pulsed laser diode for a "time-of-flight" measurement. Results of this study will be presented at a later date.

Figure 2 shows the system on top of the test section. The beams, spaced 3.5 in. apart, were expanded to approximately 1.25 in. in diameter and transmitted to a small plate carrying the two 1-cm-diam retroreflectors.

2.2 PROOF-OF-PRINCIPLE TUNNEL TEST

The test data were acquired for two cases, "tunnel-off" condition and tunnel operating at Mach 0.85. The data taken at Mach 0.85 were well suited for demonstrating feasibility since high acoustic and high-vibration levels were encountered. The "tunnel-off" data were obtained under the same physical setup as that of the "tunnel-on" data and processed by the technique discussed in Section 3.3. In both cases, the model sting movement was manually controlled as opposed to computer controlled. The tunnel-off readings were compared to angle readings made with a standard bubble inclinometer.

The tunnel evaluation was effected by placing the optics system and its associated electronics in an environmental box. A nitrogen purge avoided heat buildup emanating from the electronics and the laser. The massive environmental chamber was bolted to the top of the test section. The high acoustic and vibration levels were isolated by commercially available lead/foam mats and pneumatic vibration isolators. These isolation techniques inside the environmental box produced no detectable error contribution attributable to acoustic and structural vibrations.

The sting support system at the rear of the test section moves downward (or upward) to approximate a model rotation around a point several feet from this support mechanism. For conventional tunnel testing, the absolute location of the model rotation point need not be known because of the large physical size of the test section; however, this knowledge is of prime importance for the precision required by the fixed optical setup.

From the first measurements made in the tunnel it was found that the forward motion of the model point of rotation (versus pitch angle) was greater than anticipated, therefore negating the increase in pitch measurement range that could be obtained by setting the light beams at a predetermined incident angle. As discussed in Ref. 1, a gain in pitch measurement range is obtained when the incident beams are tilted along a line connecting the end points of the total arc swung by the retroreflectors.

An empirical relationship was derived to predict the forward motion of the model rotation point when the sting support system is used to rotate the model through an angle. This equation was used to locate the model in its pitch domain such that an angle of incidence and diameter of the light beam could be preselected to ensure a large range of pitch measurements. This equation is given by

$$y \simeq -0.24 \quad e^{0.26\alpha} - 1 \tag{2}$$

where y is the forward motion of the point of model rotation in inches and α the pitch angle. The equation is valid up to 11 deg, the maximum angle of the sting support system. A plot of Eq. (2) is shown in Fig. 3 which represents the maximum forward motion of four possible settings of the pitch rotation point.

The first proof-of-principle runs were obtained with a zero bias angle (the two incident beams were perpendicular to the tunnel centerline). This zero angle of incidence was the best compromise for measuring the largest possible pitch range.

The results of the initial measurements made with the laser interferometer were in close agreement with the data calculated by conventional wind tunnel techniques. The comparative data are tabulated in Table 1 for both air-on and air-off conditions. As evident from an evaluation of the data, the laser interferometer measurements were consistently a few hundredths of a degree larger than the tunnel computer calculated data. It is also noted that upon comparing the measurements of the change in angle, from one pitch angle to the next, there is closer agreement between the two types of measurements.

During the initial test program a number of operational problems were uncovered that necessitated improvement and modification in the design of the interferometer system. The model was positioned manually to zero angle of attack, and the interferometer system bias angle and beam diameter were set to cover the maximum pitch range possible. One problem appeared upon acquiring computer control of the model angular position. Computer control positioned the model to a slightly different axial position than was obtained during pretest setup with manual control. This caused the laser beams to fall either upstream or downstream of the retroreflectors. Predicting model position in advance proved difficult as evidenced in the "tunnel-on" data in Table I where the zero pitch angle is no longer "seen" by the optics system. At 3-deg pitch angle, the retroreflectors appear on one side of the expanded beams and fall out of the beams again at 9 deg because of the motion of the model rotation point.

The absolute signal strength received by the photodetector was another problem encountered in the tunnel setup. As pointed out in Ref. 1, the reflected light intensity at the photodetector is given by

$$I_R = I_I (1 - \beta) \left(\frac{D_R}{D_o} \right)^2 A(\theta_1) \tag{3}$$

where I_R is the reflected light intensity, I_I the incident light intensity, β the air-glass interface loss caused by reflection, D_R the retroreflector diameter, D_o the incident beam diameter, and $A(\theta_1)$ the effective apperture of the retroreflector as a function of the incident beam angle θ_1.

In practice, I_I has a Gaussian intensity distribution across the incident beam diameter further reducing the reflected light intensity when the retroreflector position is near the extreme of the incident beam. It was pointed out (Ref. 1) that large beam diameters D_o ensure that large pitch angles can be measured before the retroreflectors move out of the incident beam. However, from Eq. (3), the reflected light intensity is a function of $(D_R/D_o)^2$ indicating that large beam diameters necessarily mean low signal levels. Large diameter retroreflectors provide large signals but should not exceed 1 cm because of practical consideration of weight and physical dimensions. Beam diameters can easily be made up to 4 cm; so, with D_R = 1 cm, $(D_R/D_o)^2$ of Eq. (3) produces a factor which reduces I_R by 0.063. This factor is unacceptably low considering the reflection loss and the aperture factor $A(\theta_1)$ which further reduces the signal intensity. Furthermore, a 10-mm-diam retroreflector may be considered excessively large for installation on test models; therefore, emphasis was placed on wind tunnel measurements using 5-mm-diam retroreflectors. Here the $(D_R/D_o)^2$ factor becomes 0.016, meaning less than two percent

of the incident light is returned to the receiving lens. Figure 4 is a plot of beam diameter versus the diameter factor, clearly demonstrating the necessity of operating with smaller beam diameters.

Higher laser powers would adequately compensate for these losses but at the expense of a drastic increase of a physical size of the laser housing. It is extremely desirable to maintain the entire optics system including a laser (and laser power supply) as small as possible to ensure portability. Physical constraints imposed by the tunnel system, outside the test section walls, are also a major consideration. Again, the alternative for acquiring higher signal levels is to reduce the incident beam diameter which reduces the pitch range that can be measured, the primary reason for having larger beam diameters initially.

Precise tracking of the model (retroreflectors) would provide the means for (1) setting the peak light intensity of the incident beams on the retroreflectors; (2) reducing the incident beam diameters, limited only by the response of the tracking system; and (3) compensating for model, forward or backward, motion throughout the required test pitch range.

It was shown with the stationary optical system that, in principle, direct measurement of model pitch can be effected in a hostile optical environment. The model motion and hence the retroreflector motion inside the expanded beams proved to be greater than expected, thereby drastically limiting the range of the pitch measurement during the initial tests. A technique was developed and incorporated into the measurement system to track this motion throughout the model pitch domain.

3.0 PITCH MEASUREMENT WITH OPTICAL TRACKING

The need for a model tracking capability was demonstrated by the proof-of-principle tunnel measurements. The retroreflector movement out of the sensing beams was easily solved by providing an aiming mechanism to relocate the two sensing beams back on the retroreflectors. Mounting the optics system sideways and rotating a deflecting mirror would have accomplished this tracking requirement, however, major modifications on the environmental optics housing would have been required, so a more expedient method was chosen.

This section will discuss the same interferometric measurement as in the proof-of-principle runs but having now the capability of model tracking as it moves

through the pitch range. Since precise knowledge of the changing angle of incidence must be known, the technique and associated data processing of the scanning capability will now be discussed.

3.1 SCANNING TECHNIQUE

Rotation of the optics unit was accomplished by attaching a precision, numerically controlled, translation stage to one side of the optics package structure. The crossmember attaching the package and the isolators was a convenient attachment for the translation stage. Actuating the translation stage lowers or raises one side of the optics package where rotation occurs around the vibration isolators. Figure 5 shows this translation stage in place. To remain within the constraints of the available space inside the environmental box, the choice of a traversing unit was limited. A total travel range of 2 in. was the best traverse unit commercially available. These 2 in. of total travel produced a 4-deg rotation of the optics package. Considering the distance between the optics package on top of the test section and the test model, the 2-in. travel produced a 6-in. movement of the beams along the tunnel centerline. This scan motion completely encompasses the 4-in. forward motion of the model when the sting support unit is actuated for model pitch.

The traverse unit provided the positioning accuracy by utilizing a high-precision lead screw. Since the traverse unit is mounted on end, half the weight of the optics package rests on the lead screw. A counterweight was attached to balance out this force. In order to establish equal pressures on each pneumatic isolator, an equalizing lead weight was attached to the opposing side. The traverse stepping motor may be operated manually or by computer control to allow model tracking through a predetermined algorithm.

Motion of the traverse is sensed by recording the number of motor steps used for the bias angle change. Optics package rotation necessarily changes the path length difference between the two sensing beams; therefore, precise knowledge of the change in traverse position is necessary to compensate for its contribution to the change in path length. One step of the stepping motor moves the traverse by 0.00005 in. which corresponds to a package rotation 3×10^{-8} deg. This small angular change will not translate through the isolators. It was experimentally determined that a minimum of 500 steps would rotate the optics package repeatedly and predictably. Figure 6 shows the plot of the data with and without the equalizing weight. The 500 steps, corresponding to 9×10^{-4} deg, were found in practice to be too small for tracking purposes. Increments of 2,000 to 5,000 steps were found to be more suited for the smallest angular movement when scanning was required.

3.2 TUNNEL TRACKING CAPABILITY

It was shown (Ref. 1) that the range over which the model pitch measurement may be made is greatly affected by the incident beam angle and the radius of model rotation, R (where R is the distance from the outermost retroreflector to the point of model rotation). Also, to ensure a reasonable range of pitch measurements, the incident beams were expanded to allow the retroreflector to move along the model rotation arc and still remain inside the laser beam. It was shown in the proof-of-principle runs that the model axial position was generally not known in advance thereby negating the choices of bias angle and incident beam diameter. Because of this, the range of pitch measurements was greatly reduced or totally obliterated. By allowing the most intense portion of the incident beam to follow the retroreflector motion it is possible, in principle, to eliminate this restricted pitch measurement range. Also, since the most intense portion of the incident beam is used the maximum possible reflected light is assured. Because of the finite scan range of the optics package rotation, there still remain limits on the maximum model pitch range that can be measured. An equation was developed to facilitate selecting an appropriate incident beam bias angle in relation to the constraints imposed by the radius of model rotation and the maximum/minimum pitch angle specified by each test situation.

The equation equates the runout with the horizontal distance that can be scanned at the same height above (or below) the tunnel centerline. The runout is defined as the horizontal distance the retroreflector deviates from a tangent line (the incident beam) and the arc dictated by the rotation radius, R. The various parameters are defined in Fig. 7. The distance from the initial model horizontal position to a parallel line passing through the optics package rotation point is designated by d. From Fig. 7 the runout, Δ, is found from the difference of x_o - x. The value x is found from

$$\tan \theta_o = \frac{a_o + x}{y} \quad \text{or} \quad x = R \sin \alpha \tan \theta_o - a_o \quad \text{and} \quad x_o = R (1 - \cos \alpha)$$

Now, x_o - x may be written in terms of model rotation radius, pitch angle and bias angle, or

$$\Delta = R(1 - \cos \alpha) - R \sin \alpha \tan \theta_o - a_o \tag{4}$$

Also, a_o may be shown to be

$$a_o = \frac{R}{\cos \theta_o} - R \tag{4a}$$

Substituting a_o into Eq. (4) gives

$$\Delta = R\left[\frac{1}{\cos\theta_o} - \cos\alpha - \sin\alpha\tan\theta_o\right] \tag{5}$$

where the units specified by R will determine the units of Δ. Equation (5) is equally valid for negative pitch angles.

The horizontal scan range, Δ_s of the optics scanning device is easily determined from the tangent of the maximum and minimum angle of the optics package rotation. Again, from Fig. 7

$$\Delta_s = D(\tan\beta_2 - \tan\beta_1) \tag{6}$$

where β_2 and β_1 are the maximum and minimum angles, respectively. D is the vertical distance from the retroreflector to the optics rotation point. Rewriting the difference of the tangents using a trigonometric identity and rewriting D in terms of the radius of curvature R establishes the scan capability

$$\Delta_s = (d - R\sin\alpha)\frac{\sin(\beta_2 - \beta_1)}{\cos\beta_2\cos\beta_1} \tag{7}$$

The present capability of the rotation device is ±2 deg, so

$$\beta_2 = \theta_o + 2^\circ \qquad \text{and} \qquad \beta_1 = \theta_o - 2^\circ \tag{7a}$$

With the aid of Eqs. (7) and (5), a ratio of the radius of curvation of the model motion to the distance from the model rotation point and the optics package may be determined as

$$R/d = \frac{A}{\left\{\frac{1}{\cos\theta_o} - \cos\alpha - \sin\alpha\tan\theta_o\right\} + \left\{A\sin\alpha\right\}} \tag{8}$$

where

$$A \equiv \frac{\sin 4^\circ}{\cos(\theta_o + 2^\circ)\cos(\theta_o - 2^\circ)}$$

In this manner, with the parameters for a particular model setup using a given R/d and bias angle, θ, the pitch angle range may be determined. Figure 8 contains a plot of R/d versus pitch range for various bias angles. Further increases in pitch measurement range could be

obtained by extending the travel of the traversing device. A discussion of the increased measurement range with greater traversing capability is presented in Appendix A.

The curves in Fig. 8 show the theoretical pitch range that can be achieved under a specified test. The forward motion of the sting, because of the motion of the sting support system, is not included. Its effect is to increase the pitch measurement range since it retards the amount of runout at the higher pitch angles. A slight increase in the pitch range is also obtained from the incident beam diameter as discussed in Ref. 1. Figure 8 will determine the optimum bias angle for the pitch range specified by the test.

Actual tracking of the retroreflectors was not found to be as difficult as originally anticipated. When discrete scan steps from one position to the next were large, a clear change in signal amplitude was seen as the retroreflectors moved across the light beam. This appreciable change in signal amplitude with scanning motion facilitated tracking of the retroreflectors and could easily be automated.

Future scanning capability could provide a larger scan range than required by the pitch range of the test. The optimum bias angle is then chosen to be along a line connecting the retroreflectors at the maximum pitch angle and the minimum pitch angle or

$$\theta = \frac{(\alpha_{max} - \alpha_{min})}{2} \tag{9}$$

This ensures that the incident beams are set up symmetrically about the maximum peak of the $A(\theta_1)$ parameter (Eq. (8)). When the sting support system is the predominant pitch mechanism, the bias angle should be approximately ten percent less.

3.3 DATA PROCESSING

Control electronics and data processing equipment were located in the test cell control room with the optics system placed on top of the test cell. These locations produced a physical separation of approximately 800 ft. Figure 9 shows a flow chart of this control and data system.

The interferometer data are contained in the 15-MHz carrier frequency, and because of this excessive distance, a line driver is used to impedance-match the cable and provide a

3-db gain to compensate for cable loss. A 5-MHz bandpass amplifier, B, in the control room filters out electromagnetic noise (EMI) picked up over the 800 ft. The fringe counting readout establishes its data rate from the manually set external pulse generator. A designated number of readings, generally set at 20 samples, are averaged to minimize the effects of model or optics component oscillation. Since the data processing system utilizes the IEEE 488 standard interface bus, the addition of the optics scanning information was immediately available for processing as a result of standardized interface equipment and formats. The microcomputer also functions as the bus controller. An oscilloscope monitors the signal quality and amplitude entering the fringe counting readout. Data are processed and displayed to read model angle relative to tunnel centerline.

3.3.1 Data Processing for the Fixed System

Processing the data for the fixed nonscanning system was a simple procedure since Eq. (1) is calculated at each new model angle setting. The calculation is based on the count difference of the fringe counter so Eq. (1) is re-written in the form

$$\alpha_n = \sin^{-1}\left\{\frac{(C_o - C_n)\times F}{S}\right\} \tag{10}$$

where α_n is the model angle relative to the initial model setting at zero angle of attack. C_o is the initial count reading, C_n is the count reading at the new model angle setting, and S is the spacing between the retroreflectors in inches. F is the conversion factor that changes counts to distance and is based on the laser wavelength of 632.8 nm. Hence F is equal to 6.228×10^{-6} in./count.

3.3.2 Data Processing with Scan Capability

Reference 1 discussed the gain in pitch measurement range by providing an initial incident beam angle. Since the scanning capability may be thought of as changing this bias angle, an equation was derived based on the change in counts from the previous model angle to the new model angle. This equation is written as follows:

$$\Delta\alpha_n = \sin^{-1}\left[\sum_{1}^{n}\frac{\Delta x_n - d_o}{S}\right] - \sin^{-1}\left[\sum_{1}^{n-1}\frac{\Delta x_n - d_o}{S}\right] \tag{11}$$

where Δx is the change in distance in the direction of the incident beams as determined from the number of quarter-wavelength counts supplied by the data processing unit. Equation (11) calculates the change in each new model angle and is calculated from all the cumulative counts taken up to that point. The d_o value is given by $d_o = S \sin \theta_o$ where θ_o is the initial bias angle. Again, the subscript n indicates the model angle after each discrete model angle change. Hence the model angle relative to tunnel centerline (or the reference angle where the counters are set) is given by

$$\alpha_n = \sum_{1}^{n} \Delta\alpha_n \tag{12}$$

When the optics bias angle is changed to a new value, d changes in Eq. (11). At this point, Eq. (11) begins a new series added to the previous angle before the bias angle change. This is represented mathematically by

$$\alpha_n = \sum_{o}^{m} \sum_{1}^{n} \Delta\alpha_{nm}$$

or

$$\alpha_n = \sum_{o}^{m} \sum_{1}^{n} \left\{ \sin^{-1}\left[\frac{\sum_{1}^{n} \Delta x_n - d_m}{S}\right] - \sin^{-1}\left[\frac{\sum_{1}^{n-1} \Delta x_n - d_m}{S}\right] \right\} \tag{13}$$

where $d_m = S \sin \theta_m$ and θ_m is the new bias angle.

For computer evaluation, each angle was calculated and stored in memory after each new pitch angle change. The computer program was greatly simplified by storing the bias and model data in angular form and using only the count difference for calculating the new model or bias angle.

It can be shown that Eq. (13) transforms into angular form as follows:

$$\alpha_n = \theta_{m-1} + \sin^{-1}\left[\Delta x_n - \sin\left(\theta_m - \alpha_{n-1}\right)\right] \tag{14}$$

where θ_{m-1} is the previous bias angle, θ_m the new bias angle, and α_{n-1} the previous model pitch angle. As before Δx_n is the change in distance from the previous angular setting to the present angular setting. The computer program processing Eq. (14) is discussed in Appendix B.

The bias angle was determined from the number of pulses sent to the stepping motor driving the linear translation stage. Manual control of the traversing unit was retained to ensure the retroreflectors placement was in the center and most intense portion of the incident beams. The 15-MHz carrier frequency monitored at the input of the fringe counting unit provided the retroreflector placement information. Since the incident laser beams possess a Gaussian intensity distribution, maximizing the amplitude of the 15 MHz, as seen on the monitor, provided the optimum placement of the retroreflectors. Line drivers were necessary for transferring the stepping motor pulses over the 800-ft distance. The stepping motor output was tranmsitted to the computer system on the IEEE 488 interface bus.

3.4 TUNNEL DATA

The optics system with the model tracking capability was installed in a test requiring a pitch angle greater than 11 deg. An auxiliary pitch mechanism is required to achieve these higher pitch angles. The test required a -4 to 35-deg pitch range, hence providing a means for adequately evaluating the capability of the scan system.

The R/d value determined for this test requirement was 0.615. Using the computer program outlined in Section 3.2, a bias angle of 15 deg was established. Figure 8 is this computer evaluation from which the 15-deg bias angle was chosen. The dotted horizontal line is the R/d value dictated by the model sting arrangement.

The retroreflectors used for this test sequence were 5 mm in diameter and approximately 5 mm deep. These were imbedded in the fuselage of a 4-ft test model just in front of the vertical stabilizer. The retroreflector spacing, S, was 3.5 in. The actual bias angle and the model zero angle of attack were measured with the tunnel standard inclinometer.

A model pitch sweep with no airflow was effected in 2-deg steps. At the start of the sequence, the model pitched to some arbitrary negative value and returned to zero. The data run was started at this point with approximately 2-deg intervals taken up to 26 deg. Model tracking was easily effected by monitoring the 15-MHz carrier frequency. At each angle step, a model pitch angle was processed by the conventional technique for comparison with the direct reading laser interferometer values. Figure 10 contains a plot of the difference between the tunnel-determined angle and the laser-system-determined value versus the model angle set by the pitch mechanism.

A laboratory setup duplicating the pitch conditions of the tunnel test was established to compare these readings to the standard tunnel inclinometer. Again, pitch

measurements were made in 2-deg intervals with changes in bias angle set the same as in the tunnel run. The lower limit in setting the inclinometer to a specific angle was determined by repeatedly setting the same pitch angle as determined by the inclinometer and measuring this angle with the interferometer system. The resulting scatter in the interferometer data had a standard deviation of 0.0014 deg. A nonstabilized laser (low cost) is used in the optical system and was found to contribute little or no error caused by laser line drifts. An increase or decrease in angle of 10^{-4} deg/hr is occasionally observed because of this laser line drift. The overall interferometer error contribution was determined to be minimal based on experimental laboratory results which include the laser line drift and bias angle determinations. A comparison between the data of the inclinometer and the laser system is also plotted in Fig. 10.

Duplicating the pitch program of the tunnel test and comparing these angles to the standard inclinometer indicated a scatter in the difference readings with a standard deviation of ±0.0019 deg. It was concluded that the scatter in the calibration data was primarily attributable to the resolution limits of the inclinometer.

The tunnel data of Fig. 10 reveal a decreasing error trend with increasing model angles from zero degrees. At approximately 20 deg this trend reverses. The dotted line in the figure is an estimate of this trend. Several possibilities exist for this small difference in the tunnel evaluated angle and the interferometer evaluated angle. The pretest calibration of retroreflector spacing, the initial bias angle, and parallelism of the two beams could all contribute to this slight difference (maximum of 0.085 deg).

A similar data run was attempted with air-on condition. A short term signal dropout was present in the carrier frequency and increased in occurrence with increasing angle of attack. This momentary loss in signal produced spurious counts in the fringe counting readout system, thereby producing erroneous data. Since this problem had not been previously observed, preventative measures were not incorporated to compensate for this momentary loss of signal.

The causes of the loss of data as a result of the short-term signal dropout are as yet unresolved. It is believed this could be attributed to the abnormally high turbulence levels evidenced around this particular test model. Since smaller retroreflectors were used in the present test, compared with previous tests, the reflected beam would be smaller in diameter. The possibility exists that the turbulence levels are not as easily compensated with small retroreflectors. Nevertheless, the new data processing technique, which is being developed, is anticipated to be insensitive to the short-term signal dropout. Future efforts

will also be directed toward developing a system using only diffused light scattering from model surfaces, thereby eliminating the retroreflectors.

4.0 SUMMARY AND CONCLUSIONS

The objective of the work reported herein was to develop an optical interferometric technique for direct measurement of model pitch angle in a wind tunnel environment. The results are summarized as follows:

A laser interferometric technique using 5-mm-diam retroreflectors was demonstrated to measure model pitch angles both in the laboratory and in the AEDC Tunnel 16T. The greater-than-anticipated forward motion of the model rotation point limited the pitch measurement range from 0 to 6 deg in the proof-of-principle run. At a condition of tunnel Mach number 0.85, the system measured these pitch angles with a resolution of 0.001 deg.

Provisions for model tracking were incorporated such that pitch angles can now be measured from -5 to 40 deg with the same resolution of 0.001 deg.

This capability was shown with air-off for a pitch range from zero to 26 deg. Comparisons with the conventional angle measurement indicated an agreement for this range of 0.01 deg. A similar air-on capability is yet to be undertaken. Because of a spurious signal dropout problem, the only attempt for air-on data failed.

The primary disadvantage of this optical interferometric technique is that the measurement is relative and not absolute. An accurate reference must be available or measured independently to provide absolute pitch data. Zero angle of attack, which is known accurately from the sting and balance calibration, is adequate for this reference. Another obvious disadvantage of using retroreflectors is that model roll removes the retroreflectors from the laser beams causing loss of signal. However, retroreflectors could be placed on any roll angle, provided an adequate reference is available.

The retroreflector system has the capability of measuring instantaneous pitch angles for providing information of normal and abnormal angle-of-attack oscillations experienced at high pitch angles. Also, this system provides an alternate method for verifying the conventional technique of pitch

determination at high angles of attack where sting and model balance deflection become significant. Verification of these techniques must still be made in the wind tunnel environment before establishing this method as a routine measurement technique.

REFERENCES

1. Bomar, B. W., Goethert, W. H., Belz, R. A., and Bentley, H. T. "The Development of a Displacement Interferometer for Model Deflection Measurement." AEDC-TR-76-116 (ADA034384), January 1977.

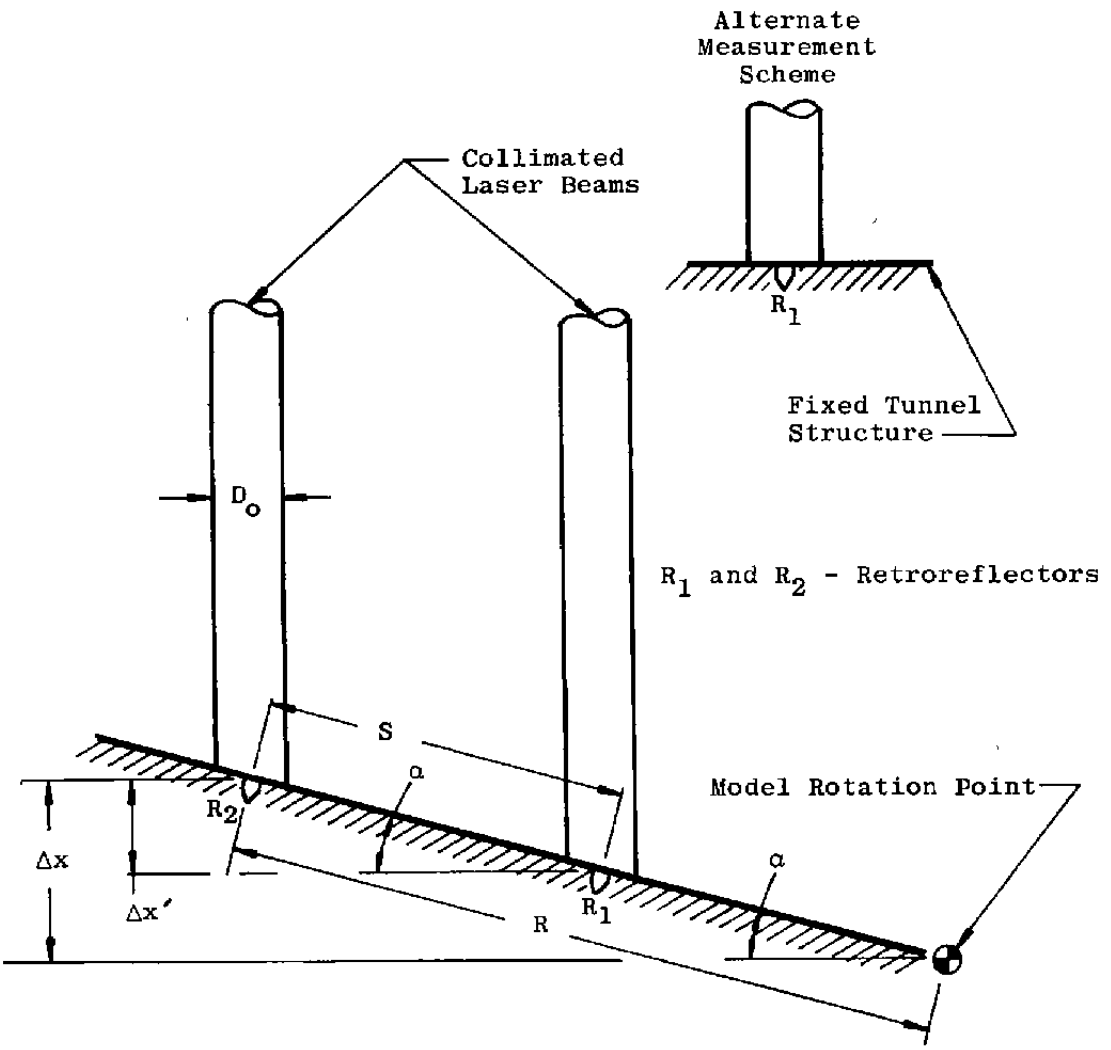

α ≡ Model Pitch Angle

S ≡ Spacing Between Retroreflectors

R = Radial Distance from Outermost Retroreflector to Point of Rotation

Figure 1. Schematic of model pitch angle measurement.

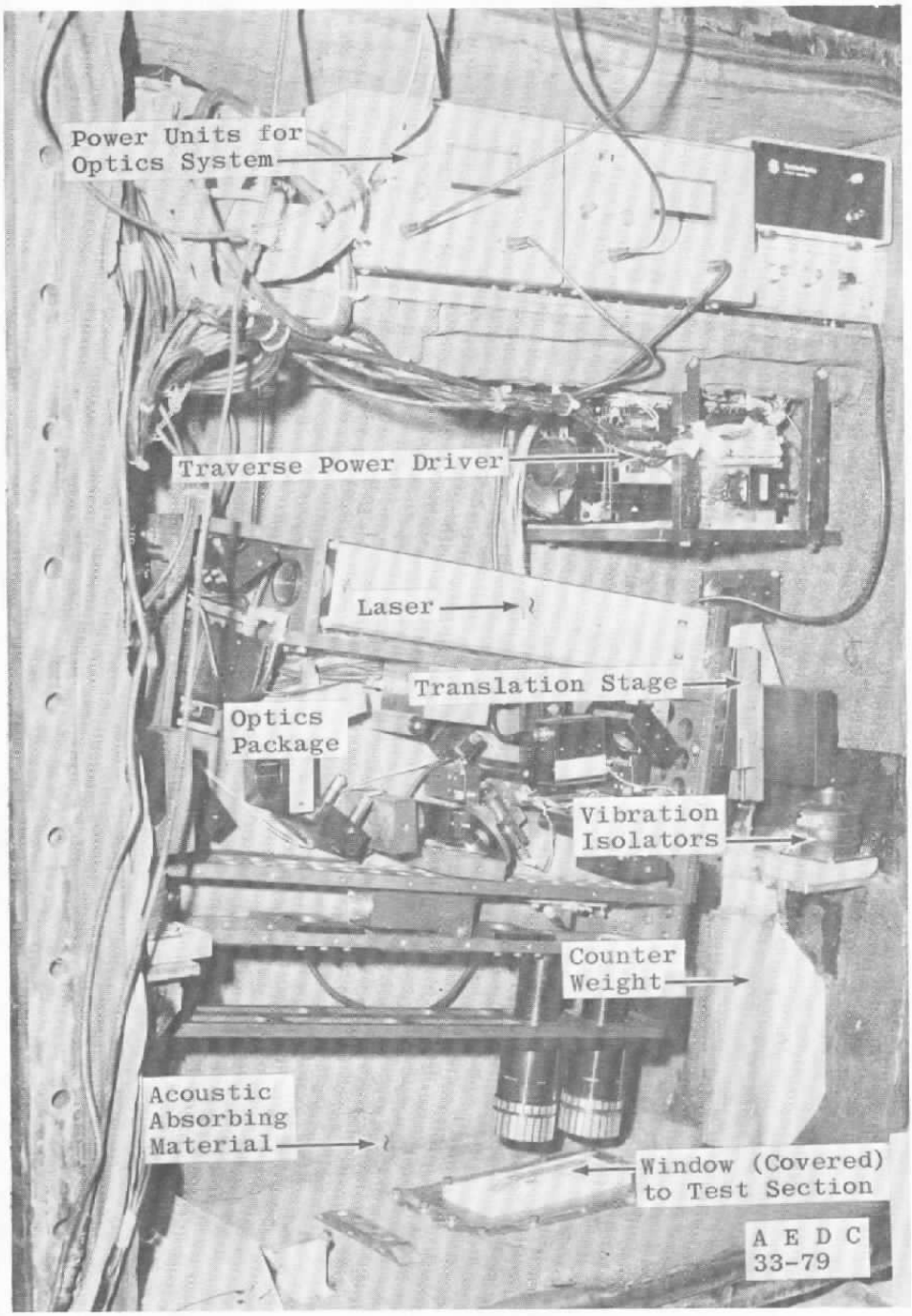

Figure 2. Laser interferometer inside environmental box on top of cart 2 test section.

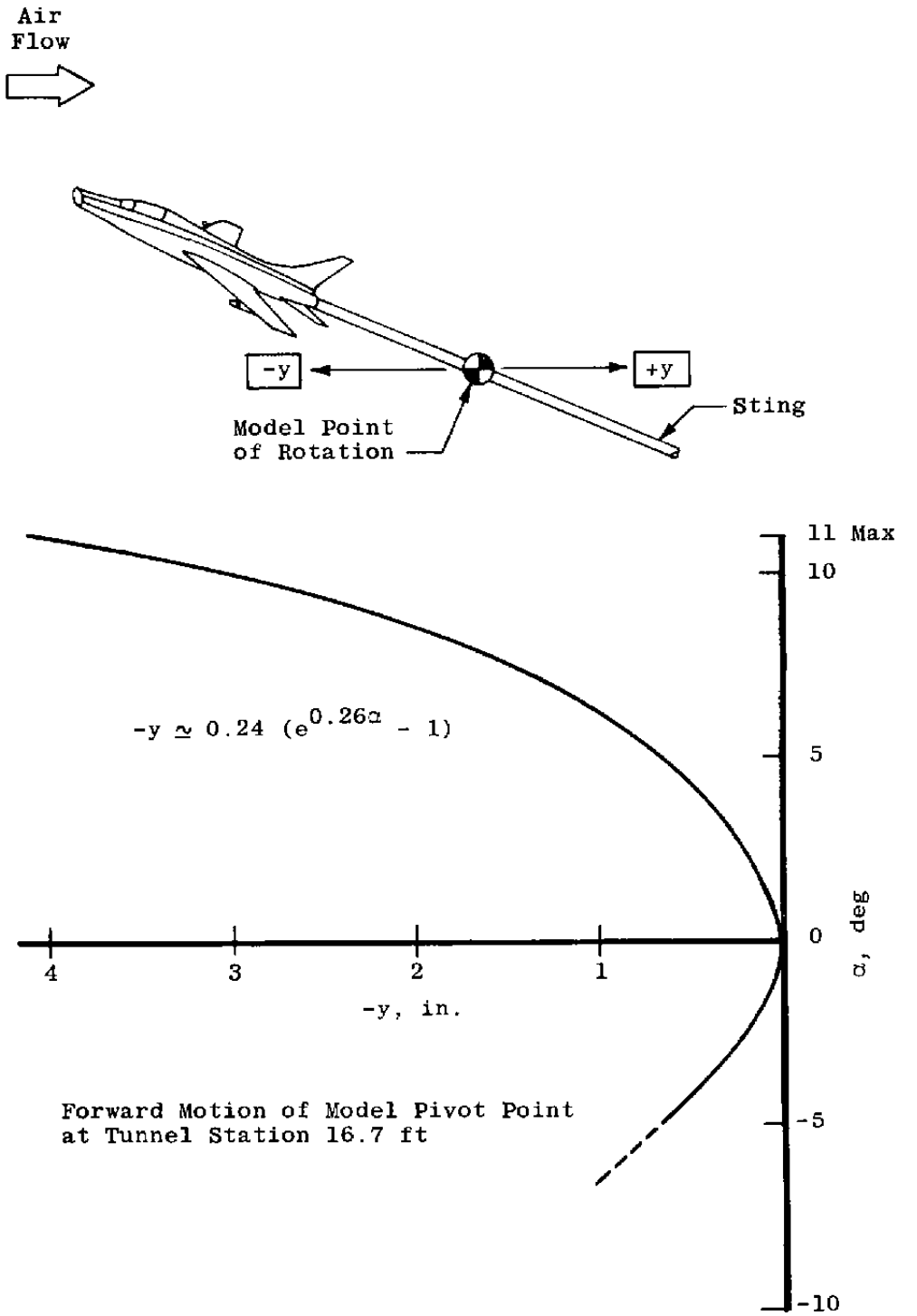

Figure 3. Model pivot point forward motion with angle setting of sting support system.

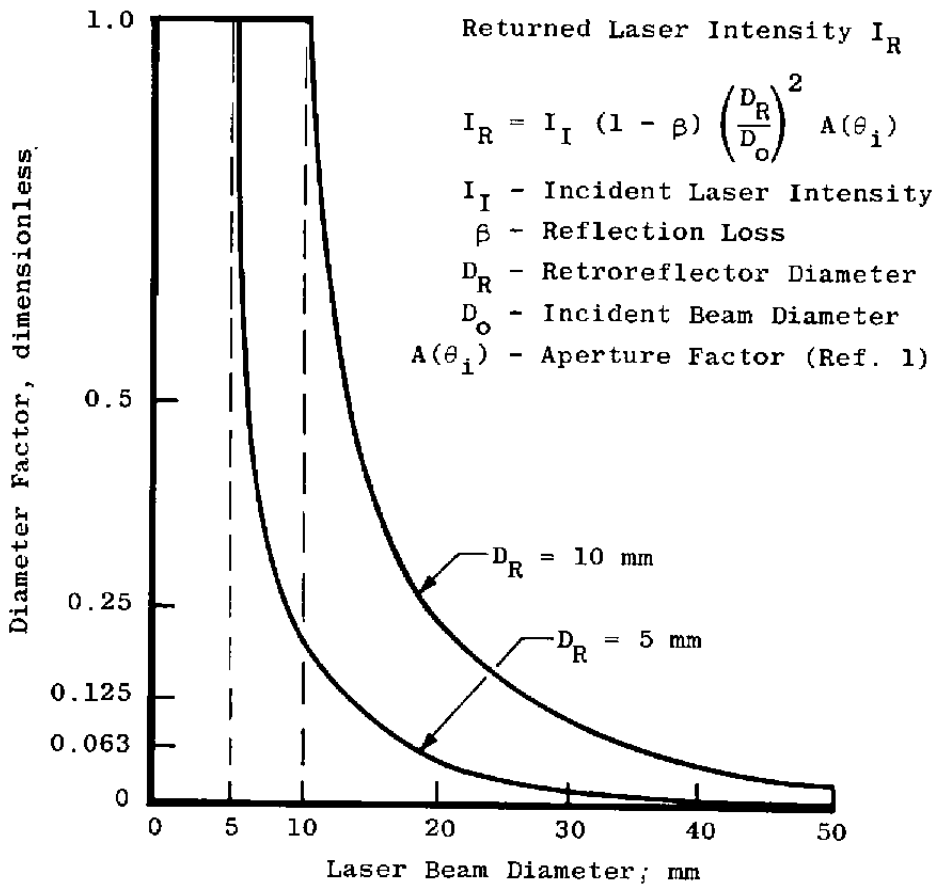

Figure 4. Diameter factor $(D_R/D_o)^2$ dependence on retroreflector size.

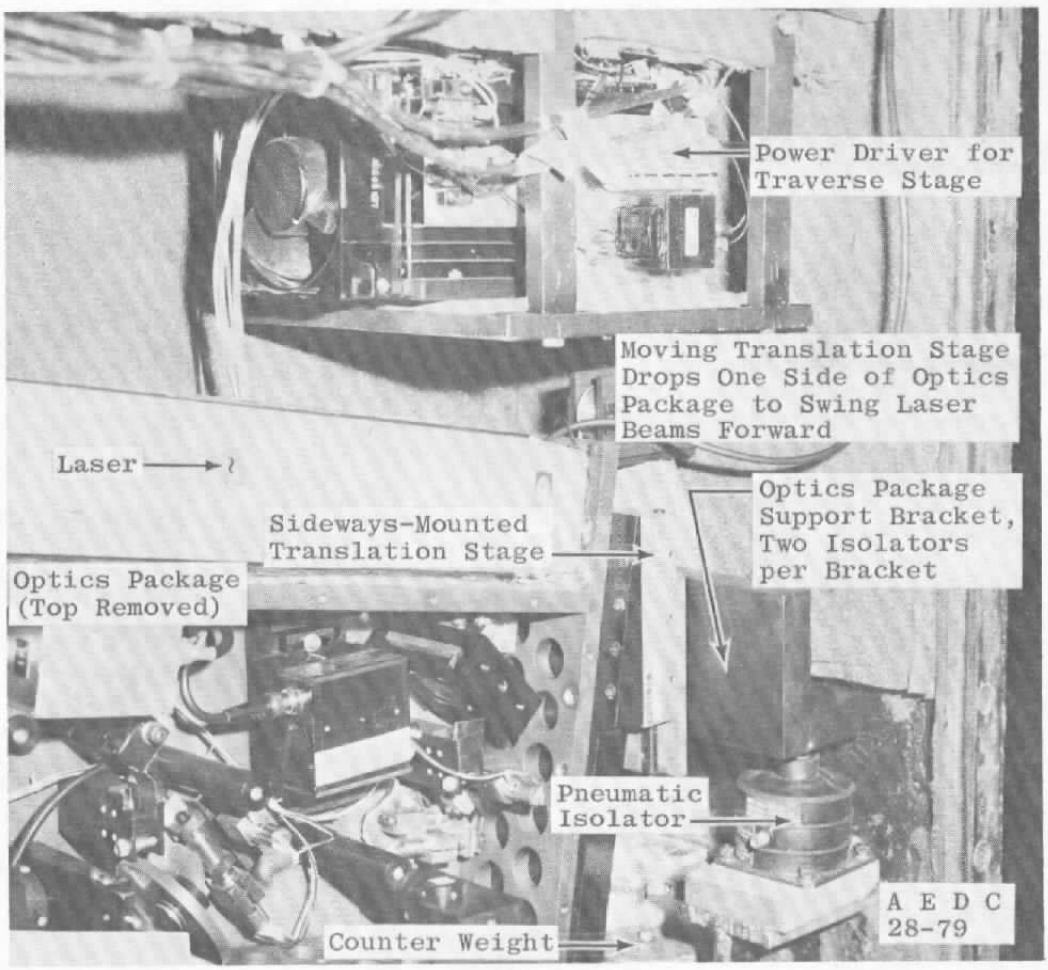

Figure 5. Optics package scanning mechanism.

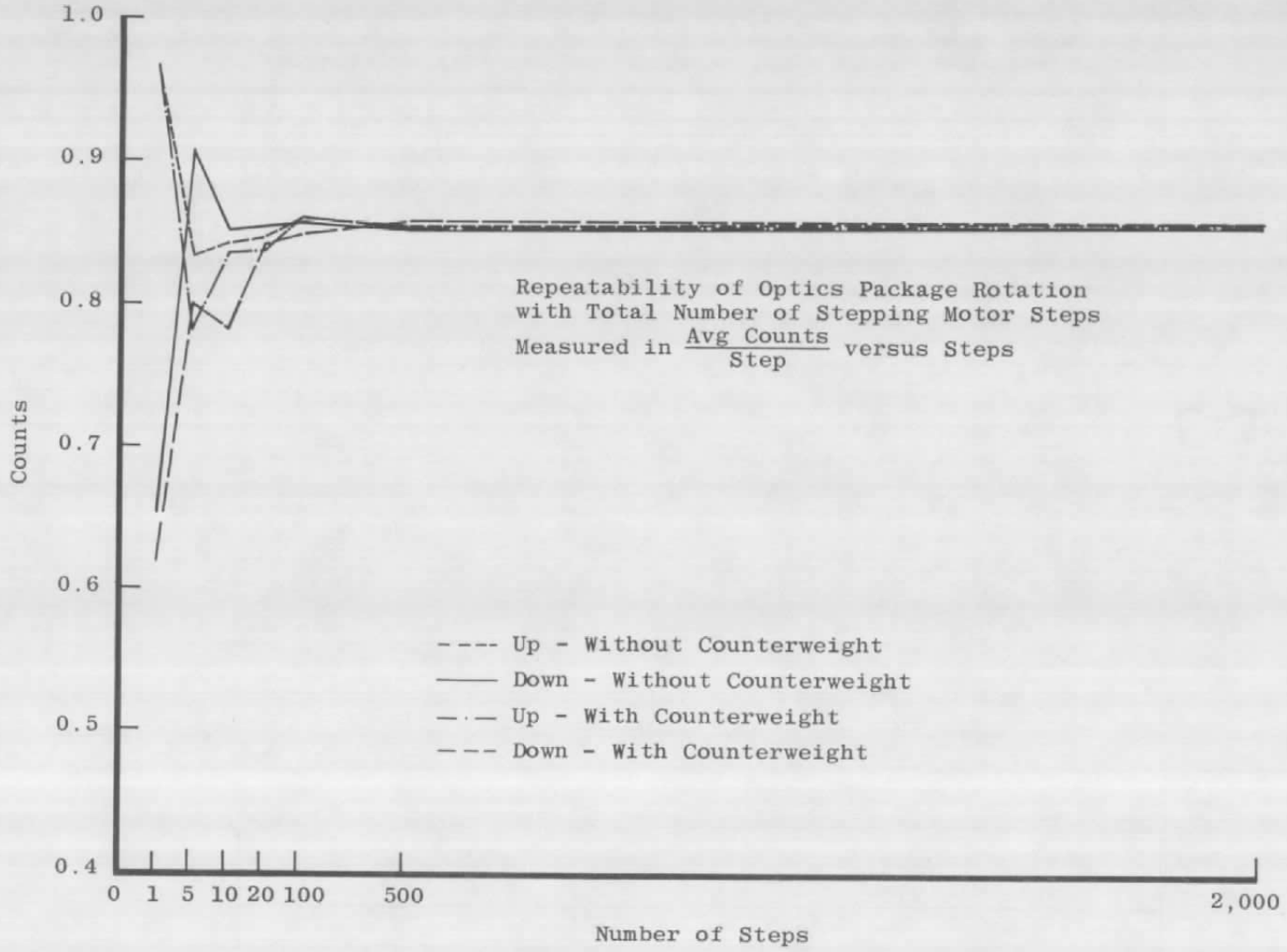

Figure 6. Repeatability of optics package rotation.

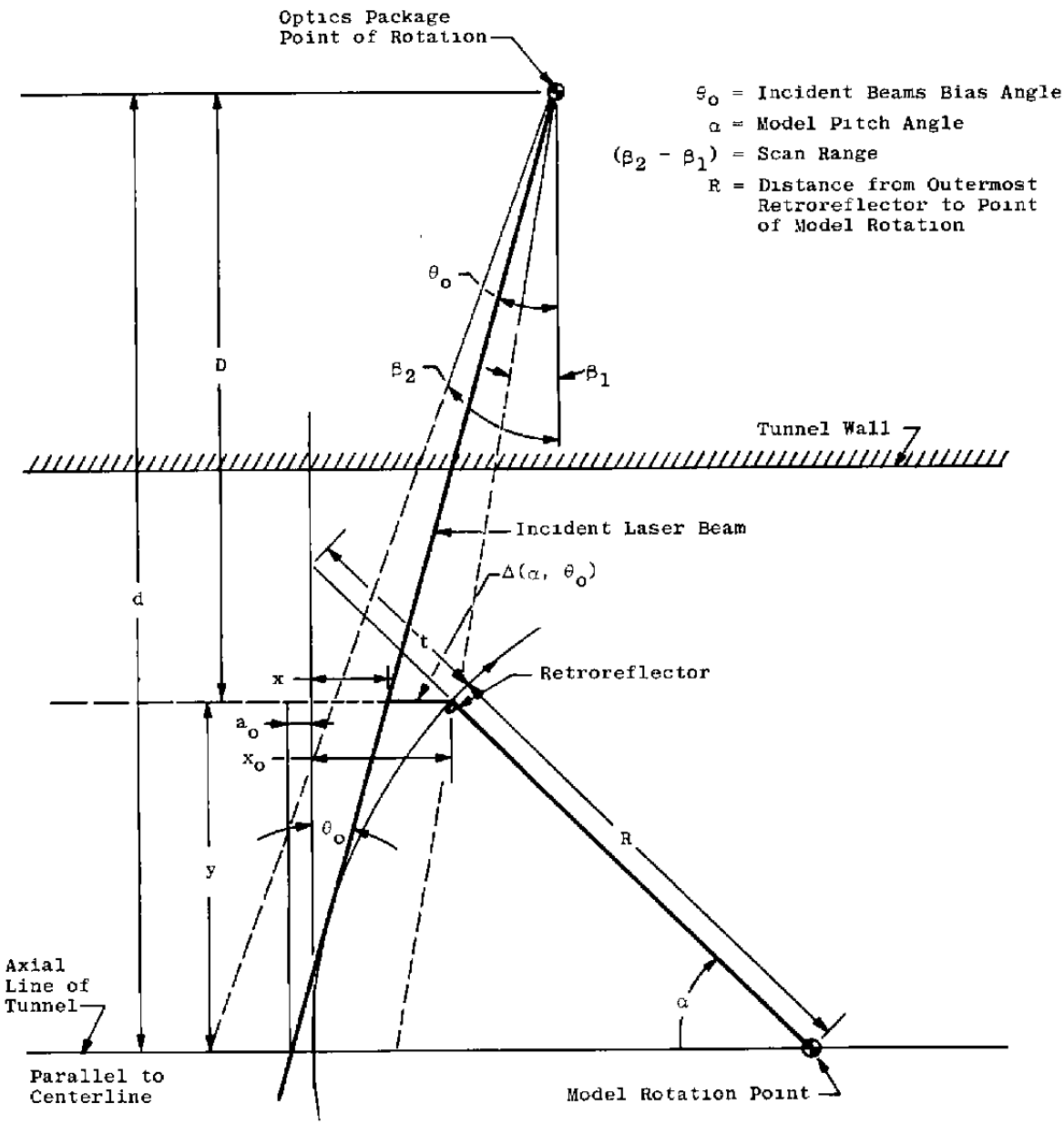

Figure 7. Defining parameters for scan and retromotion.

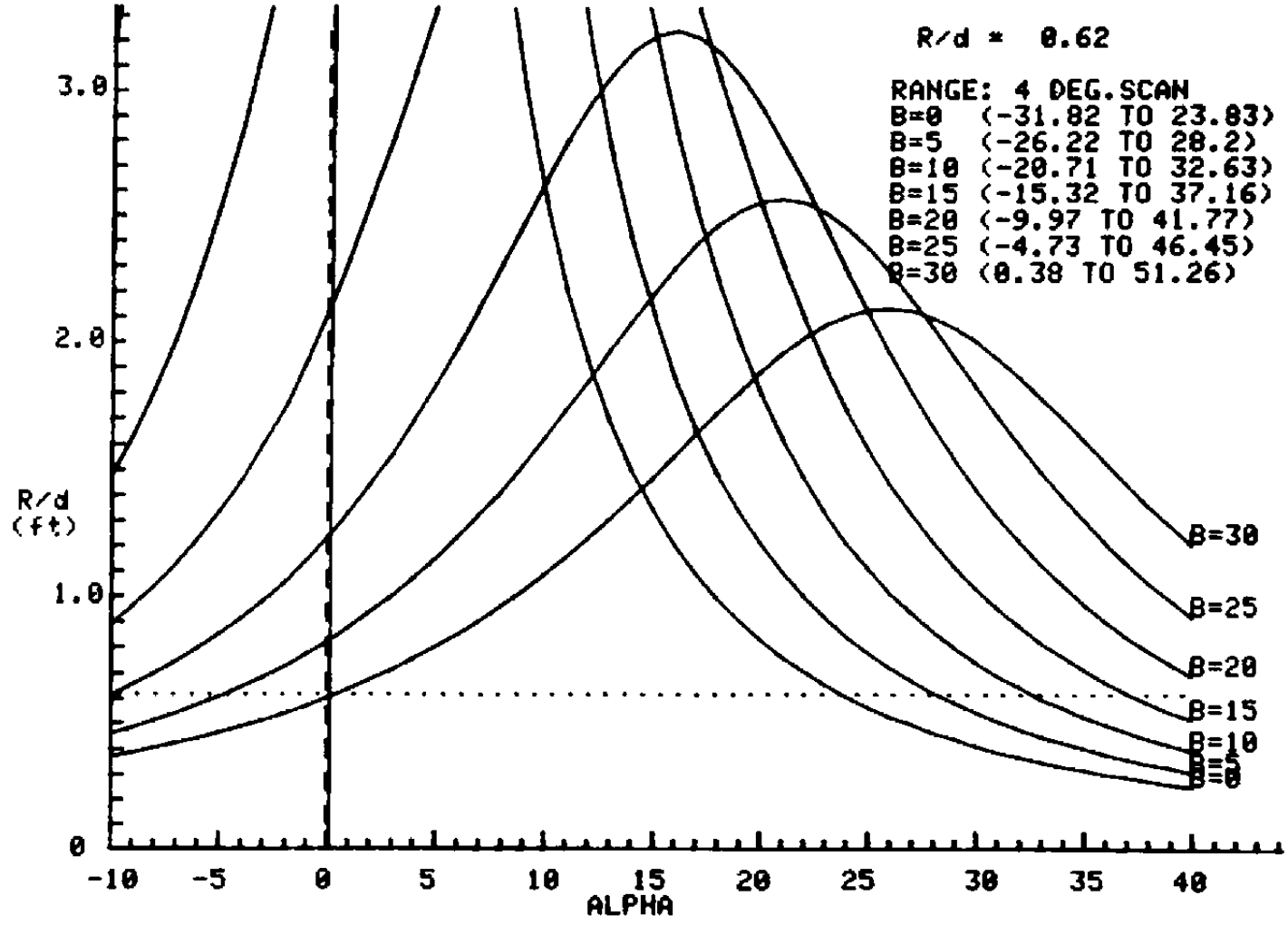

Figure 8. Pitch range as specified by bias angle B.

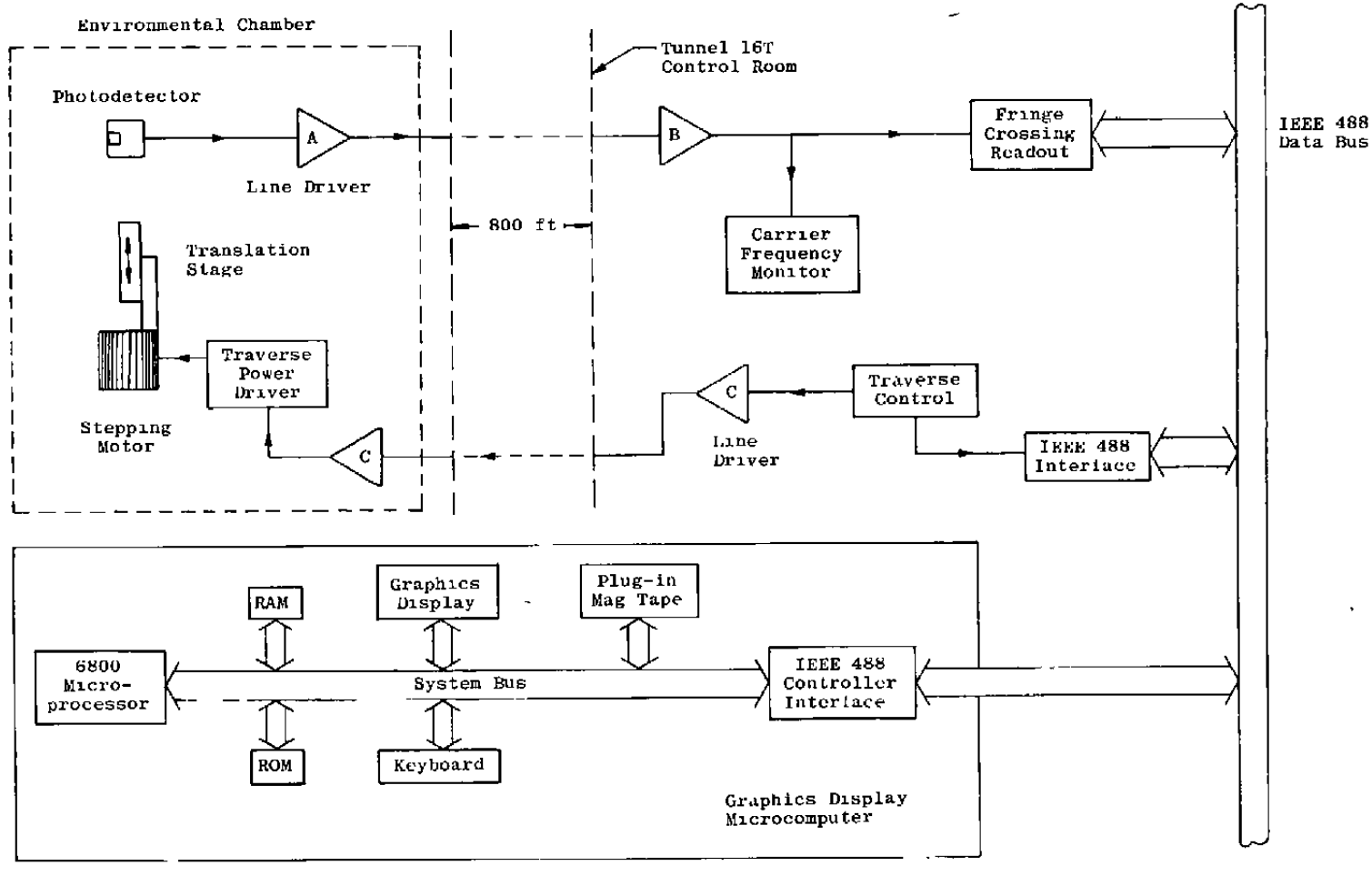

Figure 9. Data processing electronics.

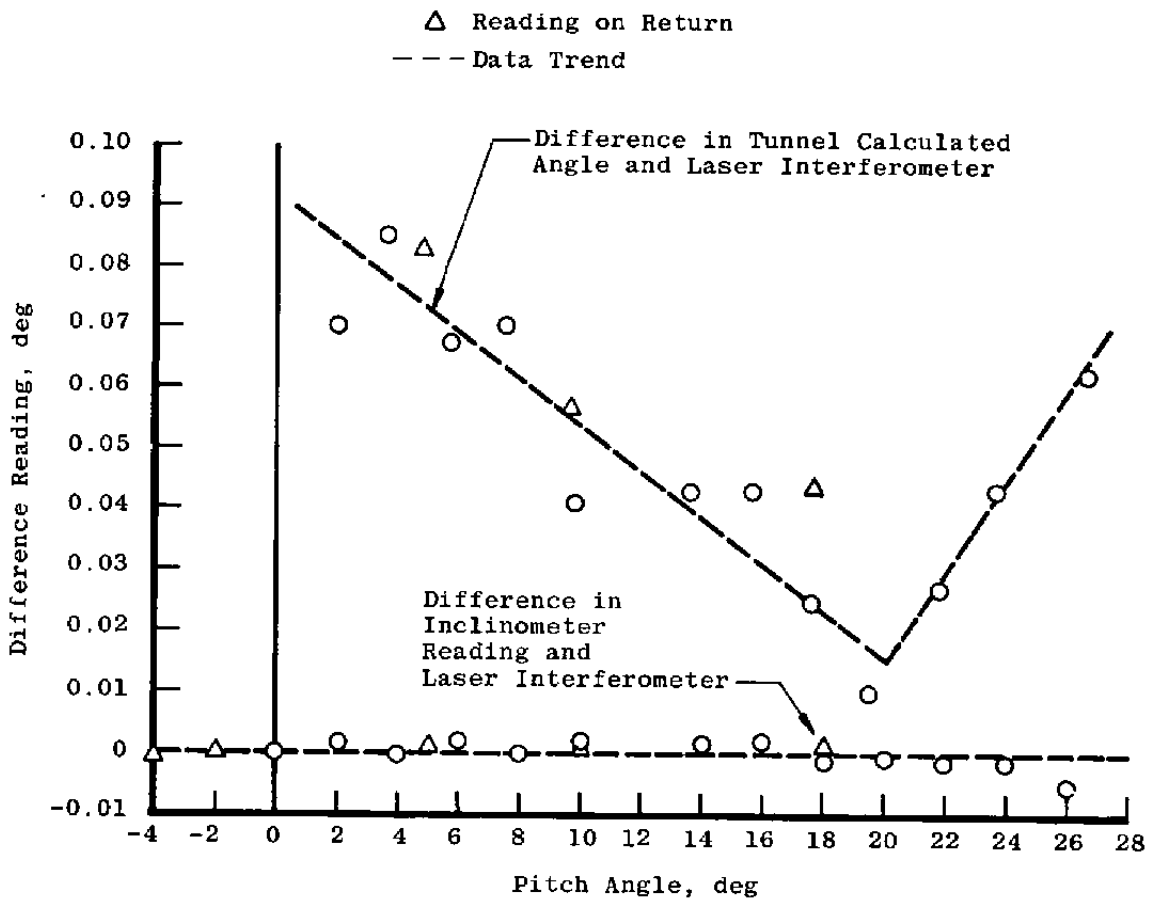

Figure 10. Angle comparison with interferometer and inclinometer/tunnel data from air-off run.

Table 1. First Proof-of-Principle Wind Tunnel Data

Tunnel Air-Off Condition

Inclinometer Measurement	Laser Measurement	
Sting Angle, deg	Measured Angle	Measured Angle Change, deg
	Ref.	
1.00	0.9993	0.9993
2.00	2.005	1.005
3.00	3.012	1.006
3.50	3.519	0.505
0	0.0024	3.516
0	Ref.	
-1.00	-1.005	1.005
-2.00	-2.016	1.011
0	Ref.	
1.00	0.9882	0.9882
2.00	2.007	1.0186
3.00	3.007	0.9992
3.50	3.5106	0.5024
0	-0.018	3.529

Tunnel Operating (Mach 0.85)

	Conventional Measurement		Laser Measurement	
Manually Set Angle, deg	Computer Calculated Angle, deg	Change in Angle, deg	Measured Angle deg	Measured Angle Change
3	Ref.		Ref.	
4	4.00	1.00	4.029	1.029
5	5.05	1.05	5.100	1.071
6	5.96	0.91	6.027	0.927
7	6.98	1.02	7.087	1.060
8	7.97	0.99	8.142	1.055
9	8.93	0.96	Sig Lost	---

APPENDIX A
COMPUTER DETERMINATION OF THE PITCH MEASUREMENT RANGE

To determine the pitch range over which interferometer data may be taken, the distance (d) from the optics package to the model rotation point (see Fig. 7) must be known. The model rotation radius, R, must also be known, but it is not as readily determined as d. An R/d value should be chosen for the pure rotational case. If the sting support is used for additional pitch, either before or after a pure rotation, it will increase the pitch measurement range. This is a consequence of the pitch support system moving the model forward. The computer program that follows quickly supplies the necessary information after the appropriate R and d values are entered into the machine.

Future scanning capability may be extended to more than ±2 deg. The only change needed in the program is to change the value of the scan angle TS in line 115 where TS is the +/- scan angle. Figure A-1 is a plot of the R/d values found from a ±3 deg scan capability (total 6 deg of scan). Comparison with Fig. 8 shows the increase in scan capability. A bias angle of B = 25 deg will allow for pitch measurements to be made from -13.21 deg to 50.66 deg where for ±2 deg the scan measurement begins at -4.73 and ends at 46.45 deg. Clearly an improvement is demonstrated.

The program in basic for these determinations follows.

```
100 REM R/d .VS. BIAS ANGLES
110 INIT
114 REM T5 IS THE PLUS-MINUS SCAN ANGLE: ENTER VALUE IN NEXT LINE
115 T5=2
120 DIM R1(51),X(51),J1(51),K(51)
130 SET DEGREES
140 C=0
150 PRINT
160 PRINT
170 PRINT
180 PRINT "          ENTER STING RADIUS R= ";
190 INPUT R
200 PRINT "          ENTER d VALUE;  d= ";
210 INPUT D
220 N=R/D
230 M=N*30
250 PAGE
260 VIEWPORT 10,130,10,100
270 AXIS 2.4,3
280 MOVE 24,-4
290 FOR Q=1 TO 100 STEP 4
300 DRAW 24,Q
310 Z=Q+2
320 MOVE 24,Z
330 NEXT Q
340 MOVE 0,M
350 FOR P=1 TO 120 STEP 2
360 DRAW P,M
```

```
370 V=P+2
380 MOVE V,M
390 NEXT P
400 MOVE -10,80
410 MOVE -10,40
420 PRINT "R/d"



430 PRINT "(ft)"
440 MOVE -4,-1
450 PRINT "0"
460 MOVE -6,29
470 PRINT "1.0"
480 MOVE -6,59
490 PRINT "2.0"
500 MOVE -6,89
510 PRINT "3.0"
520 MOVE -2,-5
530 PRINT "-10   -5     0     5     10    15    20    25     30    35"
540 MOVE 118,-5
550 PRINT "40"
560 FOR V=1 TO 10
570 V1=V*12
580 MOVE V1,0
590 DRAW V1,2
600 MOVE V1,0
610 NEXT V
620 MOVE 89,95
630 PRINT USING 635:"R/d =";N
635 IMAGE 7A,1D.2D
640 PRINT
650 PRINT "II                RANGE: ";T5*2;" DEG.SCAN"
660 FOR G=1 TO 7
670 A=5*(G-1)
680 C=A
690 B=C+T5
700 B1=C-T5
710 T=SIN(2*T5)/(COS(B)*COS(B1))
720 D1=TAN(A)
730 C1=1/COS(A)
740 K1=D1-T
750 M1=T/N-C1
760 H=0



770 DEF FNA(X)=COS(X)+K1*SIN(X)+M1
780 FOR F=1 TO 2
790 IF H=1 THEN 830
800 P1=-60
810 Q1=12
820 GO TO 850
830 P1=12
840 Q1=60
850 Z1=FNA(P1)*FNA(Q1)
860 IF Z1<0 THEN 910
```

```
870 Q1=P1
880 P1=T4
890 P1=(P1+Q1)/2
900 GO TO 850
910 U=Q1-P1
920 IF U<0.1 THEN 960
930 T4=P1
940 P1=(P1+Q1)/2
950 GO TO 850
960 IF H=1 THEN 1010
970 W=(P1+Q1)/2
980 W=INT(W*100+0.5)/100
990 H=1
1000 GO TO 1040
1010 Y1=(P1+Q1)/2
1020 Y1=INT(Y1*100+0.5)/100
1030 PRINT "II                B=";A;"","  (";W;" TO ";Y1;")"
1040 NEXT F
1050 NEXT G
1060 MOVE 24,0
1070 SCALE 1.08333,1.11111
1080 FOR G=1 TO 7
1090 A=5*(G-1)
1100 C=A
1110 B=C+T5
```

```
1120 B1=C-T5
1130 T=SIN(2*T5)/(COS(B)*COS(B1))
1140 FOR E=-4 TO 21 STEP 0.5
1150 I=(E+5)*2-1
1160 X(I)=2*(E-1)
1170 J=2*(E-1)
1180 J1(I)=J*2.4
1190 S=1/COS(A)-COS(J)-SIN(J)*TAN(A)
1200 R1(I)=T/(S+T*SIN(J))
1210 K(I)=R1(I)*30
1220 IF R1(I)<4 THEN 1250
1230 IF J1(I)>0 THEN 1250
1240 GO TO 1290
1250 IF I<>1 THEN 1280
1260 MOVE J1(I),K(I)
1270 GO TO 1290
1280 DRAW J1(I),K(I)
1290 NEXT E
1300 PRINT "B=";A
1310 HOME
1320 MOVE 0,0
1330 NEXT G
1340 MOVE 0,-5
1350 PRINT
1360 PRINT "                                        ALPHA"
1370 GO TO 1390
1380 PRINT "R/d EXCEEDS MAX. POSSIBLE: TRY AGAIN "
1390 END
```

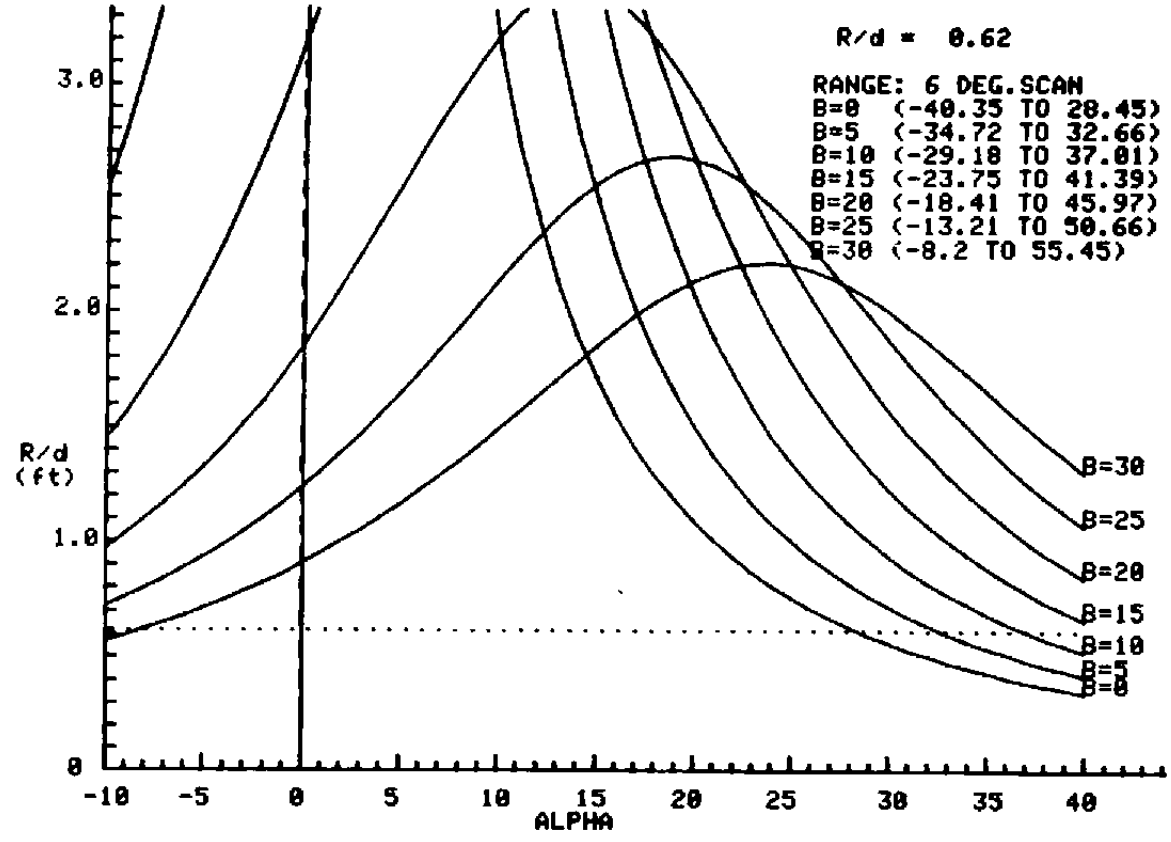

Figure A-1. Pitch range capability for scan range of ±3 deg.

APPENDIX B
COMPUTER PROGRAM FOR DATA PROCESSING

Starting the program (typing RUN) initializes the data system and acquires the initial reading from the fringe counter and traversing position counter. The program then waits for the manual command to restart the sequence by pressing the designated user definable key. The bias angle is designated by "T" in the program where Tφ represents the initial bias angle and TI the previous bias angle. F is the conversion factor discussed in Eq. (10). The present model angle is designated as P and the previous model angle PI.

Line 510 calculates the bias angle from the stepping motor pulse register where Sφ designates the initial counter reading and S the present or new reading.

The model angle is calculated in line 530. "Go sub 5,000" obtains the traverse information and "Go sub 6.000" obtains the traverse fringe counter readings. The data printout format is shown in Fig. B-1. The program file #3 appears at the beginning of the printed line. "model = " is followed by the model angle, "optics = " is followed by the optics package angle, "(Cl - C =)" provides the difference in counts from the previous reading to the present reading, and S indicates the traverse position indicator showing how far off from the original bias angle the optics package is at the end of that reading. Any reading not desired in the printout may be deleted by deleting the corresponding term in line 570.

(#3)	MODEL	Θ=	0.0000	OPTICS	Θ=13.3290	C1-C=	0.10	S=	0
(#3)	MODEL	Θ=	2.0017	OPTICS	Θ=13.4620	C1-C=	17975.95	S=	1500
(#3)	MODEL	Θ=	3.9999	OPTICS	Θ=13.6394	C1-C=	17630.95	S=	3500
(#3)	MODEL	Θ=	6.0020	OPTICS	Θ=13.8168	C1-C=	17764.70	S=	5500
(#3)	MODEL	Θ=	7.9996	OPTICS	Θ=13.9498	C1-C=	18232.25	S=	7000
(#3)	MODEL	Θ=	10.0020	OPTICS	Θ=14.0385	C1-C=	18777.55	S=	8000
(#3)	MODEL	Θ=	14.0019	OPTICS	Θ=14.0385	C1-C=	39366.00	S=	8000
(#3)	MODEL	Θ=	16.0020	OPTICS	Θ=14.0385	C1-C=	19697.05	S=	8000
(#3)	MODEL	Θ=	17.9981	OPTICS	Θ=13.9498	C1-C=	20505.15	S=	7000
(#3)	MODEL	Θ=	19.9994	OPTICS	Θ=13.8168	C1-C=	20937.35	S=	5500
(#3)	MODEL	Θ=	21.9982	OPTICS	Θ=13.6838	C1-C=	20829.95	S=	4000
(#3)	MODEL	Θ=	23.9983	OPTICS	Θ=13.4177	C1-C=	22016.85	S=	1000
(#3)	MODEL	Θ=	25.9947	OPTICS	Θ=13.1516	C1-C=	21819.45	S=	-2000
(#3)	MODEL	Θ=	18.0012	OPTICS	Θ=13.9498	C1-C=	-85572.90	S=	7000
(#3)	MODEL	Θ=	10.0013	OPTICS	Θ=14.0385	C1-C=	-79605.45	S=	8000
(#3)	MODEL	Θ=	5.0014	OPTICS	Θ=13.6838	C1-C=	-45460.35	S=	4000
(#3)	MODEL	Θ=	-0.0013	OPTICS	Θ=13.3290	C1-C=	-44927.15	S=	0
(#3)	MODEL	Θ=	-2.0004	OPTICS	Θ=13.1517	C1-C=	-17392.15	S=	-1999
(#3)	MODEL	Θ=	-3.9993	OPTICS	Θ=12.9742	C1-C=	-17239.80	S=	-4000

Model Angle, deg | Incidence Angle, deg | Interferometer Count Difference | Scan Position Indicator

Calibration Data: Same Model Angle and Optics Scan Position as Tunnel Run

Figure B-1. Data printout format.

```
1 INIT
2 SET DEGREES
3 P1=0
4 T0=15
5 T1=15
6 DIM R(20)
7 GOSUB 1000
8 F=6.328E-5/(4*2.54)
9 D=3.516
10 SET KEY
11 WAIT
24 GOSUB 1030
25 RETURN
28 GOSUB 500
29 RETURN
500 GOSUB 5000
510 T=T0-ATN((S0-S)*5.0E-5/32.283)
515 S5=S1-S
520 GOSUB 6000
530 P=T+ASN((C1-C)*F/D-SIN(T1-P1))
535 M=C1-C
536 S1=S
540 C1=C
550 T1=T
560 P1=P
570 PRINT USING 575:"(@3) MODEL 0=",+P1,"OPTICS 0=",T1,"C1-C=",M,"S=",S
575 IMAGE 13A,3D.4D,3X,9A,2D.4D,2X,5A,7D.2D,2X,2A,7D
580 RETURN
1000 GOSUB 5000
1010 S0=S
1015 S1=S
1030 GOSUB 6000
1040 C1=C

1050 RETURN
5000 PRINT @15,32:"1"
5010 INPUT @15,32:S
5015 S=-S
5020 PRINT @15,32:"0"
5030 RETURN
6000 INPUT @3,32:29
6010 INPUT @3,32:R
6020 C=0
6030 FOR I=1 TO 20
6040 C=C+R(I)
6050 NEXT I
6060 C=C/20
6070 RETURN
```

Figure B-1. Concluded.

NOMENCLATURE

A	Defined by Eq. (8)
$A(\theta_1)$	Effective retroapperture, function of light incident angle
a_o	Defined by Eq. (4a)
C, C_o, C_n	Counts from readout unit; equal to $\lambda/4$
D_o	Diameter, incident beam
D_R	Diameter, retroreflector
d	Distance between model rotation point and optics package
$d_o, (d_m)$	Bias angle factor or $d_o = S \sin \theta_o$ ($d_m = S \sin \theta_m$)
F	Conversion factor, $F = 6.228 \times 10^{-6}$ in./count
I_I	Incident light intensity
I_R	Reflected light intensity
R	Radial distance from model rotation point to outer retroreflector
S	Spacing between retroreflectors
y	Coordinate through centerline of tunnel
a, a_n, a_{n-i}	Model angle
β	Air-glass interface loss
β_1, β_2	Scan angles, minimum/maximum, respectively, Eq. (7a)
Δ	Runout, distance from arc moving by retroreflector to laser beam
Δ_s	Horizontal scan range

Δx, Δx_n	Optical path length change
θ_i	Incident beam angle
$\theta, \theta_m, \theta_{m-1}$	Bias angles
θ_o	Initial bias angle
λ	Laser wavelength